TRANSIENT OPTICAL ABSORPTION IN MAGNESIUM-DOPED LITHIUM NIOBATE

By

DONALD JAMES DAVIS

Bachelor of Arts

Thiel College

Greenville, Pennsylvania

1987

Submitted to the Faculty of the
Graduate College of the
Oklahoma State University
in partial fulfillment of
the requirements for
the Degree of
MASTER OF SCIENCE
July, 1989

TRANSIENT OPTICAL ABSORPTION

IN MAGNESIUM-DOPED

LITHIUM NIOBATE

Thesis Approved:

Larry E. Halliburton
Thesis Advisor

Craig Allison

[illegible]

Norman N. Durham
Dean of the Graduate College

ACKNOWLEDGEMENTS

I would like to thank my advisor, Dr. L.E. Halliburton, for his advice and support throughout this project. I would also like to thank Dr. S.W.S. McKeever and Dr. Craig Y. Allison for serving on my thesis committee and providing many helpful suggestions.

Many other people also contributed to the success of this thesis. I would like to thank Dr. Mahendra Jani for his friendship, advice and help with the calibration of the monochromator. I would also like to thank Dr. Reza Hantehzadeh for his suggestions and encouragement, Mr. Micheal Scripsick for sharing an unquenchable thirst for knowledge, and Mr. Jim Allen for his excellent advice. I am deeply indebted to Mr. Henry John and Mr. Gene Schemeling for their assistance and helpful suggestions. I also want to thank Dr. Donald Yeh for the use of the quartz-iodine lamp used in this study.

Most importantly, I would like to thank my wife Pam for her love, support, and encouragement during this project. Her understanding and infinite patience with me when I had to work late in the lab are greatly appreciated.

This work was supported by the Physics Department of Oklahoma State University.

TABLE OF CONTENTS

Chapter		Page
I.	INTRODUCTION	1
	Stoichiometry	2
	Crystal Structure	3
	Optical Damage	5
	Scope of this Study	8
II.	EXPERIMENTAL PROCEDURE	10
	Introduction	10
	Sample	10
	Cryostat	12
	Optical Slit	12
	High Energy Electron Source	14
	Lamp	14
	Optical Multichannel Analyzer	14
	Calibration	15
	Triggering	17
	Data Collection	17
	Infrared Absorption Measurements	18
III.	DATA ANALYSIS	22
IV.	EXPERIMENTAL RESULTS AND DISCUSSION	29
	Transient Optical Absorption Above 200 K	29
	Transient Optical Absorption Below 200 K	36
V.	SUMMARY	41
REFERENCES		43

LIST OF TABLES

Table		Page
I.	Room Temperature Photoluminescence Peaks in Nd: YAG	21
II.	Summary of Transient Optical Absorption Results in 5% Magnesium-Doped Lithium Niobate	42

LIST OF FIGURES

Figure		Page
1.	Stacking sequence of interstitial ions in lithium niobate above and below the Curie temperature	4
2.	Positions of niobium and lithium atoms in the oxygen octahedron	6
3.	Experimental setup used to induce and measure transient optical absorption	11
4.	Optical cryostat used for irradiations above temperatures of 200 K	13
5.	Spectral sensitivity curve for Model 1421 detector	16
6.	Spectral sensitivity curve for S-1 type photomultiplier tube and lamp output with 850 nm optical filter	20
7.	OMA III keystroke program to calculate average absorbance at the peak of each scan in a decay process	24
8.	IBM Basic program to calculate lifetime from absorbance versus time data	26
9.	IBM Basic program to calculate activation energy from lifetime versus temperature data	28
10.	Decay of the 550 nm optical absorption band at 300 K for 5% magnesium-doped lithium niobate	30
11.	Natural logarithm of absorption versus time for the 550 nm optical absorption band in 5% magnesium-doped lithium niobate	32
12.	Arrhenius plot of lifetime versus temperature data above 200 K	33
13.	Effect of lamp intensity of lifetime of decay for the 550 nm band at 300 K for 5% magnesium-doped lithium niobate	34

Figure Page

14. Decay of the 1200 nm optical absorption band at 23 K for 5% magnesium-doped lithium niobate .. 37

15. Decay of the 550 nm optical absorption band at 50 K for 5% magnesium-doped lithium niobate 38

16. Arrhenium plot of lifetime versus temperature data below 200 K 39

CHAPTER I

INTRODUCTION

Lithium niobate has a wide variety of properties which are useful in device applications in the electro-optic industry. Lithium niobate can be fabricated into a wide variety of devices including modulators, switches, and optical signal processors [1]. Its linear and nonlinear optical properties can be enhanced or limited by doping with appropriate impurity atoms [2]. Lithium niobate can be used to frequency double infrared lasers [3] into the visible part of the spectrum and can also be used as a laser host material [4].

Lithium niobate is not found in nature. It was first described by Zachariasen [5] in 1928 but it was not studied extensively until after Ballman [6] demonstrated that it could be grown by the Czochralski technique in 1965. Crystals of lithium niobate grown by this technique have higher optical quality and can be grown faster and larger than by other methods.

In the Czochralski technique, the reactants, namely Li_2O and Nb_2O_5, or crushed lithium niobate crystals, are contained in a platinum crucible. This, in turn, is placed in an induction-heated furnace and taken to near the melting

point. A seed crystal attached to the end of the pull rod is dipped into the melt, and then simultaneously rotated and pulled from the melt. To help prevent the crystal from cracking due to thermal stress, there is usually an after-heater located immediately above the induction furnace to permit a slow cooling of the crystal to room temperature.

Stoichiometry

The chemistry of lithium niobate is interesting in that crystals can be grown which vary significantly from the stoichiometric composition. Lithium niobate belongs to the Li_2O-Nb_2O_5 system whose solid-liquid curve on the phase diagram [7] does not have a maximum at 50 mole% LiO_2 as required for stoichiometric congruent growth. The congruent melt composition of lithium niobate was determined by Chow et al. [8] to between 48.50 and 48.60 mole% of LiO_2. In a congruent melt, the crystal and the melt have the same composition during the growth, thus resulting in uniform crystals. Crystals grown from a stoichiometric melt will have an inhomogeneous composition along the growth direction.

A parameter commonly used to characterize the stoichiometry of lithium niobate is the ratio of Li to Nb atoms. The Li/Nb ratio can be expressed as the ratio of the concentrations of lithium to niobium atoms or the ratio of the lithium atom concentration to the sum of the lithium and niobium atom concentrations. The latter definition gives the result in mole percent.

Many physical properties of lithium niobate depend on the Li/Nb ratio including: the Curie temperature, refractive indices, second harmonic phase matching temperature, UV absorption edge, x-ray luminescence, and the NMR linewidths of the Li and Nb atoms [9].

Crystal Structure

Lithium niobate has a complex perovskite-like structure [10]. The oxygen atoms form an octahedral system by being arranged in a distorted hexagonal closed-packed structure. The niobium and lithium atoms are located in the interstitial region of the oxygen octahedron. The interstials are stacked in the following order: niobium, vacancy, lithium, niobium, vacancy, lithium, and so on in the +c direction. In lithium niobate's paraelectric phase, which occurs above its Curie temperature of about 1200°C, the lithium atoms lie in the plane of the oxygen layer. In the ferroeclectric phase which is below the Curie temperature, elastic forces displace the lithium atoms in the +c direction above the plane of the oxygen ions. Figure 1 schematically depicts the stacking of the interstitials above and below the Curie temperature.

At room temperature, lithium niobate belongs to the 3m (C_{3v} in Schoenflies notation) symmetry point group and the R_{3c} space group [10]. This point group is characterized by a threefold rotation axis and three vertical mirror planes. In this point group it is possible to select either the

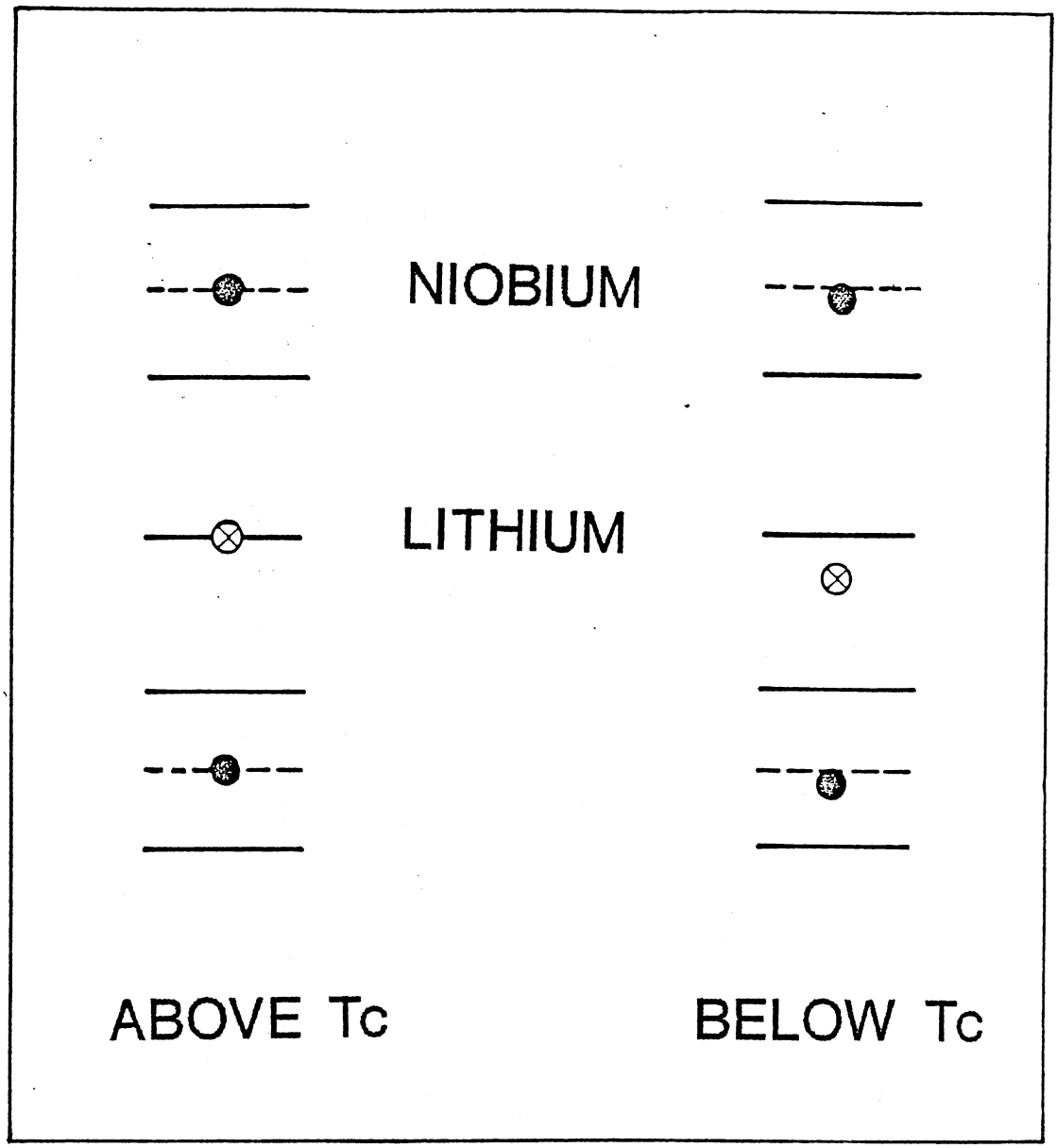

Figure 1. Stacking sequence of interstitial ions in lithium niobate above and below the Curie temperature.

hexagonal or rhombohedral unit cell. The former will be used for our discussion.

The hexagonal unit cell in lithium niobate contains six formula weights and the c axis is defined as the threefold rotational symmetry axis. The interatomic distances and unit cell parameters are shown in Figure 2.

Optical Damage

Optically induced changes in the refractive indices of a material is known as the photorefractive effect or optical damage. This laser-induced effect in lithium niobate can cause severe beam divergence thus limiting the use of these crystals as modulators, switches, and second harmonic generators. While optical damage is devastating from a device viewpoint, it can be utilized to holographically store information. Optical data storage is essential in the operation of a practical optical computer.

In 1969 Chen [11] proposed a model for the photorefractive effect in lithium niobate. He suggested that electrons in the crystal are excited by the laser beam and can migrate to different trapping sites leaving positive ionized centers in the illuminated region of the crystal. These electrons move out of the illuminated region and are then "frozen" in place by the small dark conductivity of the crystal. The separation of charge between the positive ionized centers and the "frozen" electrons establishes an electrostatic field on the order of 10^5 volts/meter. This field

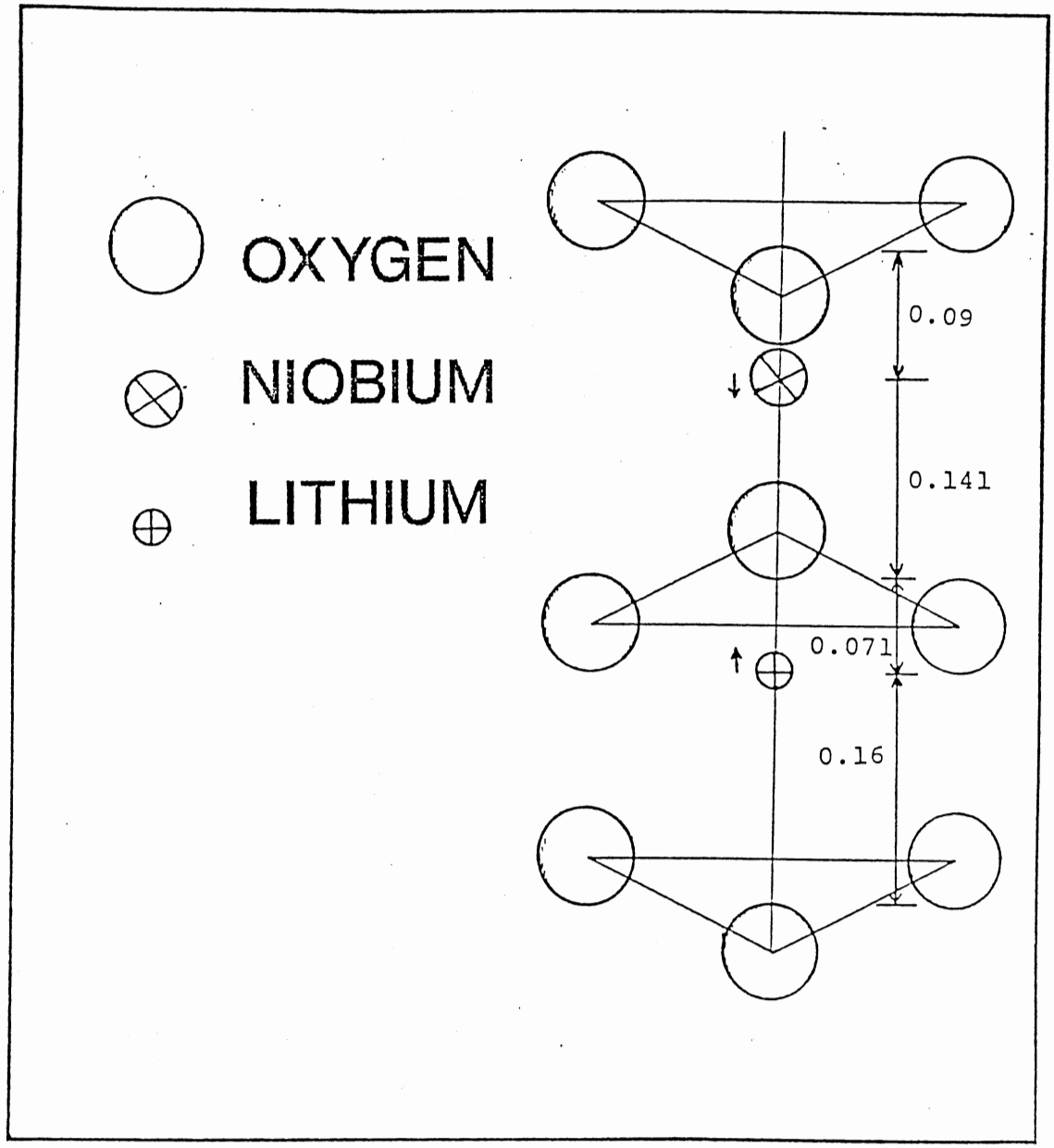

Figure 2. Positions of niobium and lithium atoms in the oxygen octahedron.

produces a change in the refractive indices by the linear electro-optic effect. The resulting inhomogeneity in the refractive indices scatters the laser beam causing the beam to diverge.

The photorefractive effect in lithium niobate can be diminished by several methods including doping the melt with magnesium oxide during crystal growth, changing the Li/Nb ratio of a grown crystal, and periodic poling of a crystal. Bryan et al. [12] observed that optical damage in lithium niobate can be reduced significantly by doping crystals with greater than 4.5% MgO. The existence of a magnesium doping level where the resistance to optical damage is enhanced is known as the threshold effect. Bryan et al. [12] measured a significant increase in the photoconductivity of their magnesium-doped samples above threshold compared to undoped samples. They attributed the resistance to optical damage to the increase in the photoconductivity.

Holman et al. [13] demonstrated that optical damage could be reduced by the out-diffusion of lithium oxide from lithium niobate crystals. This technique involves heating the crystal in the presence of another solid containing mixed lithium niobate phases. An advantage of this method of reducing optical damage is that it can also be used to produce high quality optical waveguides.

Periodic poling of lithium niobate can also increase its resistance to optical damage [14,15]. A few mole percent of chromium or yttrium is added to the melt and a

periodic electrical signal is applied to the crucible during crystal growth. A crystal grown under these conditions has alternating ferroelectric domains with periodicity on the order of ten microns. Periodically poled lithium niobate allows second harmonic phase matching independent of the crystal's birefringence.

Transient optical damage was reported by Holman et al. [16] in out-diffused lithium niobate optical waveguides. A waveguide subjected to a 10 mW cw laser beam with a wavelength of 488 nm suffered an almost complete loss of power output in 0.25 seconds. About 80% of the output was recovered in one second and the original output was observed in four seconds. This process occurs faster for shorter wavelengths and slower for longer wavelengths. The process occurs faster for a higher laser power. They suggest that this effect is caused by a laser-induced inhomogeneity in the refractive indices which scatters the light beam. The refractive indices change with time until a steady-state condition is observed. In this state, the refractive indices are changed uniformly throughout the crystal so that the original output is measured.

Scope of this Study

In this study, we investigate the optical response of magnesium-doped lithium niobate crystals when subjected to ionizing radiation. The goal of this research is to characterize the optical absorption spectra induced by fast

pulses of 1-MeV electrons and to develop defect models explaining the data. Applications of this work include predicting the radiation response of devices using lithium niobate. Also, our study will lead to a better understanding of the formation and decay kinetics of defects in this important material.

CHAPTER II

EXPERIMENTAL PROCEDURE

Introduction

Transient optical absorption spectra were induced and measured using the experimental setup shown schematically in Figure 3. In this chapter, we describe the instrumentation and procedures used in this investigation. First, we describe the source and the composition of the lithium niobate sample. Second, the hardware used to collect the data is described in detail. Finally, the calibration, triggering, and data collection procedures are discussed.

Sample

The magnesium-doped lithium niobate sample used in this study was grown by Crystal Technology, Palo Alto, CA for the McDonnell Douglas Company. This was a stoichiometric sample with 5% MgO added to the melt. The size of this sample was 2 mm x 9mm x 16 mm in the x, y, and z directions, respectively. This sample had been polished prior to the beginning of our study.

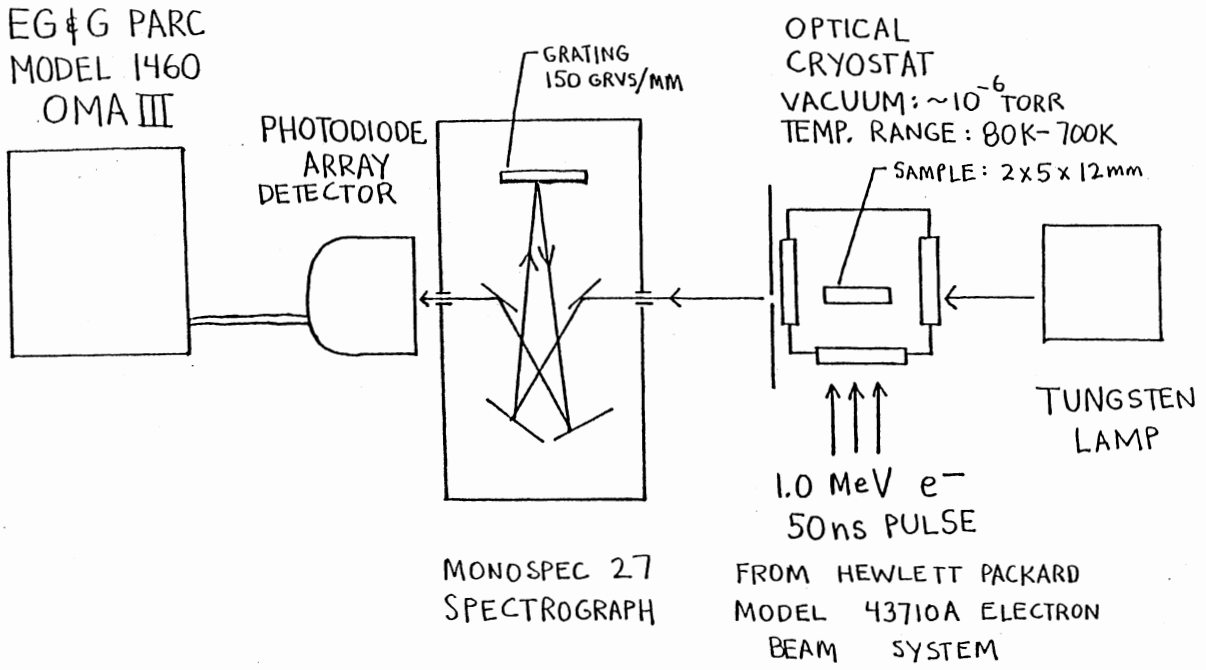

Figure 3. Experimental setup used to induce and measure transient optical absorption.

Cryostat

The lithium niobate samples were placed in an optical cryostat which was built in the Physics and Chemistry Instrument Shop at Oklahoma State University. A diagram of this instrument is shown in Figure 4. To maintain temperatures of about 200 K, dry ice flakes (solid carbon dioxide) were poured into the well of the cryostat. Temperatures around 0°C were obtained by pouring crushed ice into the well of the cryostat. A cartridge-type heater was inserted into the well of the cryostat to obtain temperatures above room temperatures. The voltage across the heater was adjusted by a Variac to obtain the desired temperature. The temperature was varied from 200 K to 500 K using these techniques. The temperature was monitored by a chromel-alumel (K-type) thermocouple mounted on one of the sample mount screws. The thermocouple was connected to an Omega MJC electronic ice point then to a Hewlett-Packard digital multimeter. The cryostat was continuously pumped to a vacuum of about five microtorr using a diffusion pump.

Optical Slit

A 0.5-mm slit mounted on a modified bar-type lens holder was placed in front of the exit window of the cryostat to limit the light output. The slit was positioned so that only light passing through the crystal near the irradiated face passed through the slit. The penetration depth of the electrons in the crystal is on the order of 1 mm. This

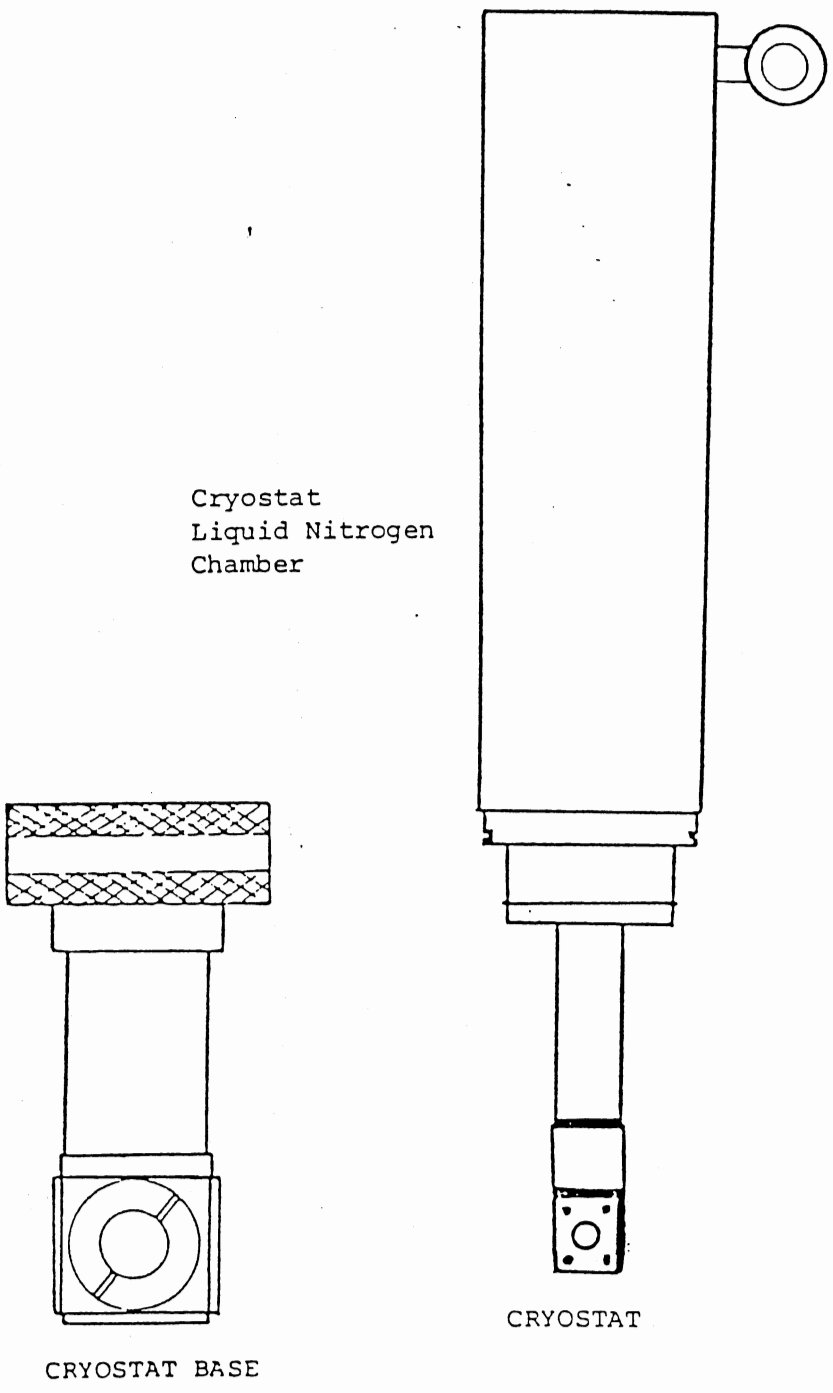

Figure 4. Optical cryostat used for irradiations above temperatures of 200 K.

was determined by irradiating the crystal at liquid nitrogen temperature and examining the coloration with the naked eye.

High Energy Electron Source

The source of the ionizing radiation was a Hewlett-Packard Model 43710A Electron Beam System. This system is composed of a pulser connected by a cable bundle to a console containing the control and support equipment. Included in the console are the high voltage power supply, the digital delay generator, the trigger amplifier, the gas regulators, and other hardware. Pressing the button on the trigger initiation circuit will produce a 50 nanosecond pulse of 1.0 MeV electrons at the emitting surface of the pulser.

Lamp

A Bausch and Lomb 45-watt tungsten lamp was used as the source of light for all the optical absorption experiments described in this study. The tungsten lamp has a broad output spectrum extending from about 300 nm through 1800 nm.

Optical Multichannel Analyzer

The absorption measurements in the visible and near infrared were performed using an EG&G Princeton Applied Research Optical Multichannel Analyzer (OMA III) with a Model 1421 Recticon photodiode array detector. The Jarrell-Ash MonoSpec 27 spectrograph used was a Czerny-Turner configuration with a 150 micron entrance slit. A grating with

150 grooves per millimeter and blazed at 450 nanometers was used in this study.

The OMA III system consists of the EG&G Model 1218 Detector Controller and EG&G Model 1460 System Processor. The detector controller provides power, temperature, and scan control for the detector array. The system processor, via a touch-screen monitor, allows human interface to the OMA III system and the means for data acquisition, manipulation, display, and storage.

The Recticon detector is an array of 1,024 silicon photodiodes. The detector is thermo-electrically cooled to 0°C to limit the dark current due to thermally generated charge carriers and is purged with nitrogen gas to prevent condensation on the photodiode array. The exposure time, the length of time that light is allowed to integrate on the detector, was set to a minimum of 17 milliseconds.

Calibration

It is essential that the OMA's Recticon detector be calibrated for intensity and wavelength since the detector's spectral response is not linear as indicated in Figure 5. This figure shows points representing data supplied by the manufacturer with a smooth line passing through them. The Recticon detector has a useful wavelength range from 200 nm to about 850 nm. The detector was calibrated for a wavelength range from 253 nanometers to 810 nanometers using an

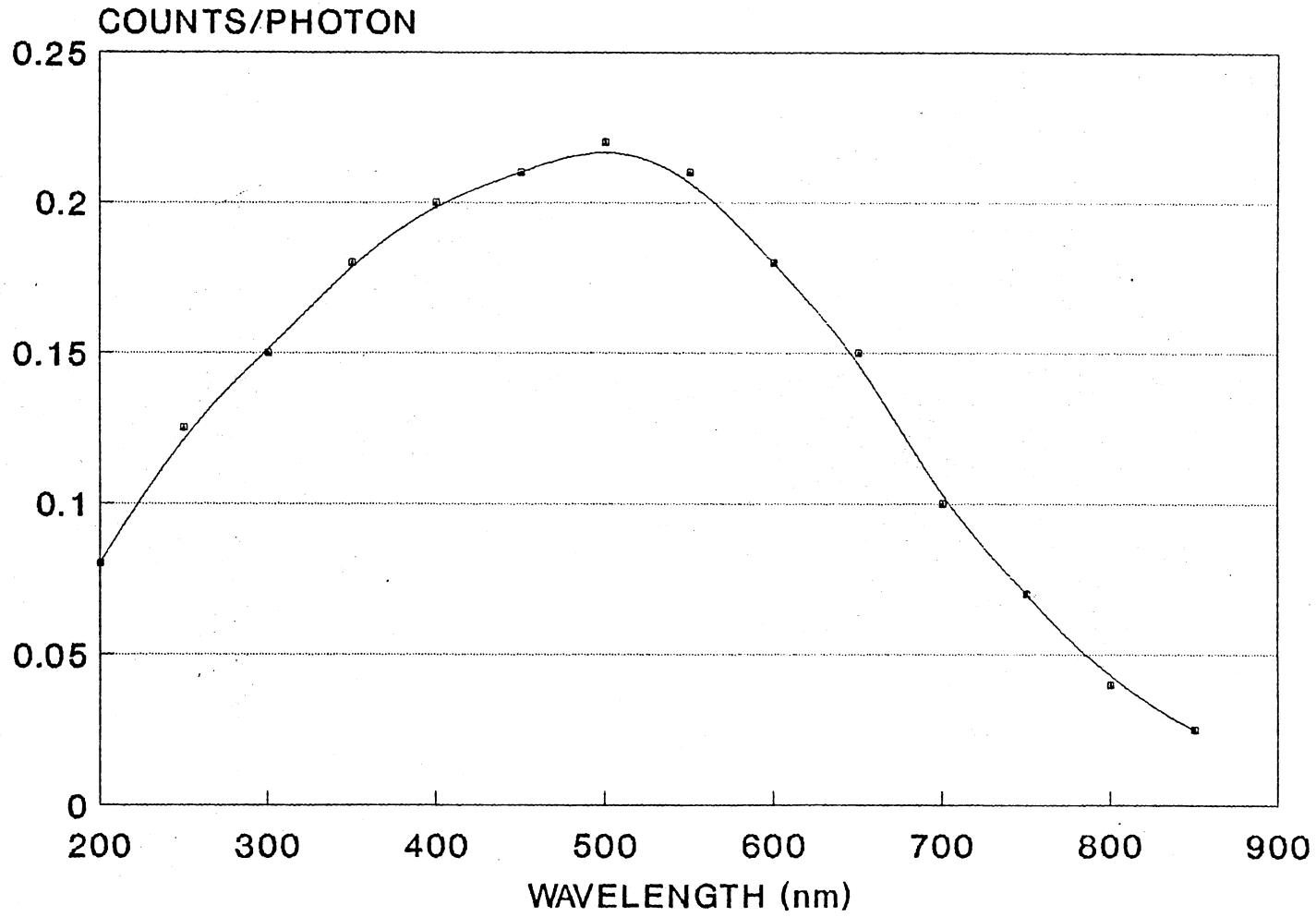

Figure 5. Spectral sensitivity curve for Model 1421 detector.

Oriel mercury-argon discharge lamp. The detector was calibrated for intensity using a quartz-iodine lamp traceable to the National Bureau of Standards. The OMA III has built-in software to accommodate these calibrations.

Triggering

A trigger pulse is sent from the electron beam system to the OMA III to initiate data collection. The event trigger input of the OMA III is connected via a coaxial cable to the delay monitor output of the digital delay generator on the console of the electron beam system. A data acquisition mode on the OMA III is selected which begins data collection when a pulse from the Febetron reaches the event trigger input.

Data Collection

The experimental procedure for producing and measuring transient optical absorption will now be described. First, the light from the tungsten lamp passed through the crystal and optical system and was incident on the detector. This spectrum was stored by the OMA III as background light. The electron beam system was then fired, producing a pulse of high-energy electrons incident on the crystal sample. Simultaneously, a signal was sent to the OMA III to begin data acquisition. Data was collected in the form of a series of consecutive exposures (i.e., light-gathering periods) following the radiation pulse with each exposure cover-

ing the spectrum from 250 nm to 810 nm. Typically, 90 exposures were accumulated after each irradiation. Each exposure was background corrected as it was collected. To accommodate longer data acquisition times, the OMA III's software allows a user-selected number of exposures to be ignored. The data collected during an ignored exposure is discarded by the OMA III.

Infrared Absorption Measurements

Absorption measurements in the infrared near 1200 nm were performed using a Bausch and Lomb monochromater and a Thorn EMI (type S1) photomultiplier tube. The grating in the monochromater had 675 grooves per millimeter. The photomultiplier was operated at 1.4 kilovolts and thermoelectrically cooled to -25°C. A Model 4093 Nicolet digital oscilloscope with a Model 4175 dual channel plug-in was used to monitor the output of the photomultiplier. For this part of the study the sample was placed in the cryostat of an Air Products closed cycle helium refrigerator. The temperature of the sample could then be varied from about 20 K to 300 K. An Air Products Model ADP model K temperature controller was used to regulate the temperature. A long pass optical filter with a 50% transmission point at 850 nm was placed in front of the monochromater to cut off the visible part of the spectrum. This was essential since the monochromater's short path length and simple configuration made it prone to second-order effects.

A spectral sensitivity curve for the S1 type photomultiplier tube is shown in Figure 6. This figure shows points representing data supplied by the manufacturer with a smooth line passing through them. Note that the sensitivity is very low near 1200 nm. Despite this, the light signal observed on the scope was typically ten times greater than the dark current signal. Also shown in this figure is the uncalibrated output of the tungsten lamp after it has passed through a long pass optical filter with a 50% transmission point at 850 nm. The points represent data collected by scanning the monochromater and measuring the light level with the photomultiplier tube. The curve is a smooth line passing through the points.

The monochromater was calibrated by observing deviations between observed and known room temperature photoluminescence peaks of Nd:YAG. For this, an alexandrite laser was used to pump a Nd:YAG crystal at a wavelength of about 780 nm. The luminescence passed through a Spex monochromater, then the Bausch and Lomb monochromater, and was detected by a lead sulfide detector whose output was displayed on an oscilloscope. The Spex monochromater was adjusted to a luminescence peak then the other monochromater was adjusted until the signal was maximized. Table I summarizes these experimental results and shows the known values of Nd:YAG photoluminescence. The results show that the Bausch and Lomb monochromater was very close to calibration and needed only a small correction of 5 nm.

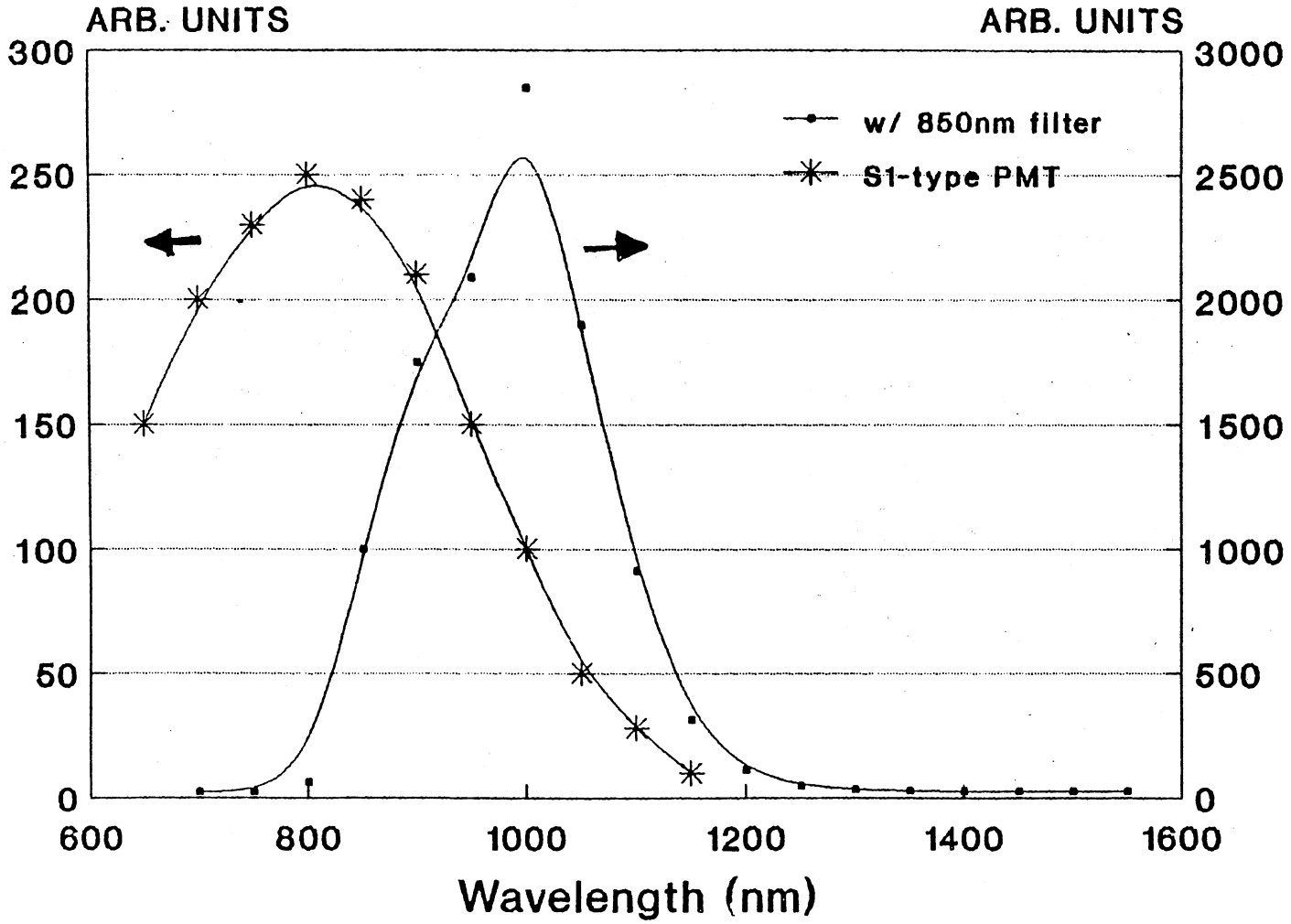

Figure 6. Spectral sensitivity curve for S-1 type photomultiplier tube and lamp output with 850 nm optical filter.

TABLE I

ROOM TEMPERATURE PHOTOLUMINESCENCE PEAKS
IN Nd: YAG

Reported by Koechner [17] (nm)	Measured with Spex monochromater (nm)	Measured with Bausch & Lomb monochromater (nm)
1064.1	1064	1070
1318.8	1316	1325
1333.8	1338	1338
1356.4	1350	1350
1414.0	1408	1410
1444.0	1440	1440

To collect data, the tungsten lamp and the photomultiplier tube were switched on and a signal was observed on the scope. Normal triggering was selected and triggering occurred by pressing the scope's trigger button. The high-energy electron source was then fired and the light level was monitored as a function of time.

CHAPTER III

DATA ANALYSIS

In this chapter we will present the methods by which the transient optical absorption data were analyzed. First, we describe how the data were extracted from the OMA III. Second, a model for the time dependence of the absorption data is discussed. Finally, the Arrhenius equation and temperature dependence of the decay of the optical absorption is discussed.

Data stored with the OMA III can be manipulated by means of keystroke programs. In general, keystroke programming on the OMA III is similar in nature to entering the keystrokes into the memory of a programmable calculator. This allows one to automatically execute frequently used sequences of commands thus eliminating operator error with the added benefit of increased speed. The keystroke menu on the OMA III provides the user the means to edit, run, list, and store programs.

In Chapter II, we described how 90 exposures would be collected during a typical optical absorption decay following the high-energy electron pulse. The first step in analyzing these data is to convert them to an absorbance-versus-time set of data at a particular wavelength (usually

chosen to be the peak of the induced absorption curves). The pixel corresponding to the peak of the induced absorption curves is determined by a visual examination of the raw data. Then the keystroke program listed in Figure 7 sequentially steps through the stored sets of data (i.e., exposures) and determines, in each case, the average absorbance for a group of ten pixels centered about this peak. Because the exposures are equally spaced in time, this results in an array of absorbance-versus-time for the specific wavelength chosen.

Specifically, the keystroke program enters the utility menu and selects the first exposure. It then calculates the average value for the ten pixels and displays this result for two seconds. It then proceeds to the next exposure and repeats the procedure. The absorbance values and their corresponding times were entered into a notebook and used in the next stage of data analysis.

Next, a model for the optical absorption process will be presented. A pulse of high energy electrons incident on lithium niobate produces free electrons and holes throughout the crystal. Many of these free electrons and holes will be captured at various trapping sites and the resulting defects will have associated optical absorption bands. The relative amount of absorption is proportional to the number of defects.

```
1:   V1=1;
2:   UT;
3:   DO 90;
4:   NS 1;1;V1;V1;
5:   ASD 545;10;
6:   WAIT 2
7:   V1-V1+1
8:   LOOP
9:   END
```

Figure 7. OMA III keystroke program to calculate average absorbance at the peak of each scan in a decay process.

It is observed that these absorption bands decay with time and we assume first-order kinetics for this disappearance. The equation used to describe the decay of the absorption bands is

$$-d[A]/dt = K[A]$$

where [A] is the concentration of filled traps and K is the rate of decay. Integrating this equation gives

$$[A(t)] = [A_o] \exp(-t/k)$$

where k - 1/K and is called the characteristic lifetime of the decay process. The initial concentration of filled traps is $[A_o]$. This equation shows that the number of filled traps and, equivalently, the absorption bands will decrease exponentially with time. A graph of the natural logarithm of absorbance versus time will be a line whose slope is the negative reciprocal of the characteristic lifetime.

A computer program was written in IBM Basic to perform a least squares fit of the natural logarithm of absorbance versus time curve discussed in the preceding paragraph. A listing of this program is provided in Figure 8. The program reads a sequential file of absorbances evenly spaced in time, calculates the natural logarithms, performs a least squares fit, then outputs the lifetime.

```
 10        'LEAST SQUARES FIT PROGRAM I
 20        INPUT " ENTER NAME OF DATA FILE"; DATAFILE$
 30        OPEN DATAFILE$ FOR INPUT AS #1
 40        INPUT #1,N
 50        INPUT #1.MT
 60        DIM I (N), T (N)
 70        FOR J=1 TO N
 80             T(J)=J+!)*MT
 90             INPUT #1, C
100             I(J)=LOG(C)
110        NEXT J
120        S1=0
130        S2=0
140        S3=0
150        S4=0
160        S5=0
170        FOR J=1 TO N
180             S1-S1+T(J)
190             S2=S2+T(J)^2
200             S3=S3+I(J)
210             S4=S4+I(J)^2
220             S5=S5+T(J)*I(J)
230        NEXT J
240        D=N*S2-S1^2
250        M=(N*S5-S1*S3)/D
260        R-( (N*S5-S1*S3)^2)/(D*(N*S4-S3^2))
270        PRINT "LIFETIME  (secs) :";-1/M
280        PRINT "QUALITY OF FIT:";R
290        CLOSE #1
300        END
```

Figure 8. IBM Basic program to calculate lifetime from absorbance versus time data.

As with most chemical reactions, we expect the rate or time dependence of the trapping and recombination processes, and hence the optical absorption, to depend on temperature. The Arrhenius equation

$$\ln(1/k) = \ln(I) - E/k_bT$$

is an empirical result which many reactions obey. In this equation, I is the pre-exponential factor, E is the activation energy, k_b is the Boltzmann constant, and T is the temperature in degrees Kelvin. According to this equation, the rate of the reaction increases exponentially as the temperature is increased. From the above, it is apparent that a graph of ln(1/k) versus 1/T should give a straight line.

A second computer program was written in IBM Basic to perform a least squares fit of the ln(1/k) against 1/T data points. A listing of this program is given in Figure 9. The program reads a sequential file containing lifetimes and temperatures, does the required calculations, performs a least squares fit, then outputs the activation energy.

```
 10        'LEAST SQUARES FIT PROGRAM II
 20        INPUT "ENTER NAME OF DATA FILE"; DATAFILE$
 30        OPEN DATAFILE$ FOR INPUT AS #1
 40        INPUT #1, N
 50        DIM I (N),T(N)
 60        FOR J=1  TO N
 70             INPUT #1,C1
 80             I(J)=LOG(1/C1)
 90             INPUT #1,C2
100             T(J)=1000/C2
110        NEXT J
120        S1=0
130        S2=0
140        S3=0
150        S4=0
160        S5=0
170        FOR J=1  TO  N
180             S1=S1+T(J)
190             S2=S2+T(J)^2
200             S3=S3+I(J)
210             S4=S4+I(J)^2
220        S5=S5+T(J)*I(J)
230        NEXT J
240        D=N*S2-S1^2
250        M=(N*S5-S1*S3)/D
260        R=((N*S5-S1S3)^2)/(D*(N*S4-S3^2))
270        PRINT "ACTIVATION ENERGY (eV):";-  M*8.314/96
             .485
280        PRINT"QUALITY OF FIT:";R
290        CLOSE #1
300        END
```

Figure 9. IBM Basic program to calculate activation energy from lifetime-versus-temperature data.

CHAPTER IV

EXPERIMENTAL RESULTS AND DISCUSSION

When a magnesium-doped lithium niobate crystal is exposed to a pulse of ionizing radiation, two different optical absorption bands are observed. These absorption bands decay away with time even at temperatures below 40 K. The transient optical absorption bands behave quite differently in the two temperature ranges: one above a temperature of approximately 200 K and the other below a temperature of 200 K. Only one optical absorption band, peaking near 550 nm, was observed above 200 K. Absorption bands peaking near 1200 nm and 550 nm were observed below 200 K. We believe that the two bands peaking near 550 nm, one above and the other below 200 K, are from the same defect but there is no conclusive evidence to support this. Now, the experimental results will be discussed and probable defect models will be presented.

Transient Optical Absorption Above 200 K

One broad optical absorption band peaking near 550 nm is observed when the sample is irradiated above a temperature of 200 K. The time decay of this absorption band at 300 K is illustrated in Figure 10. This figure shows four

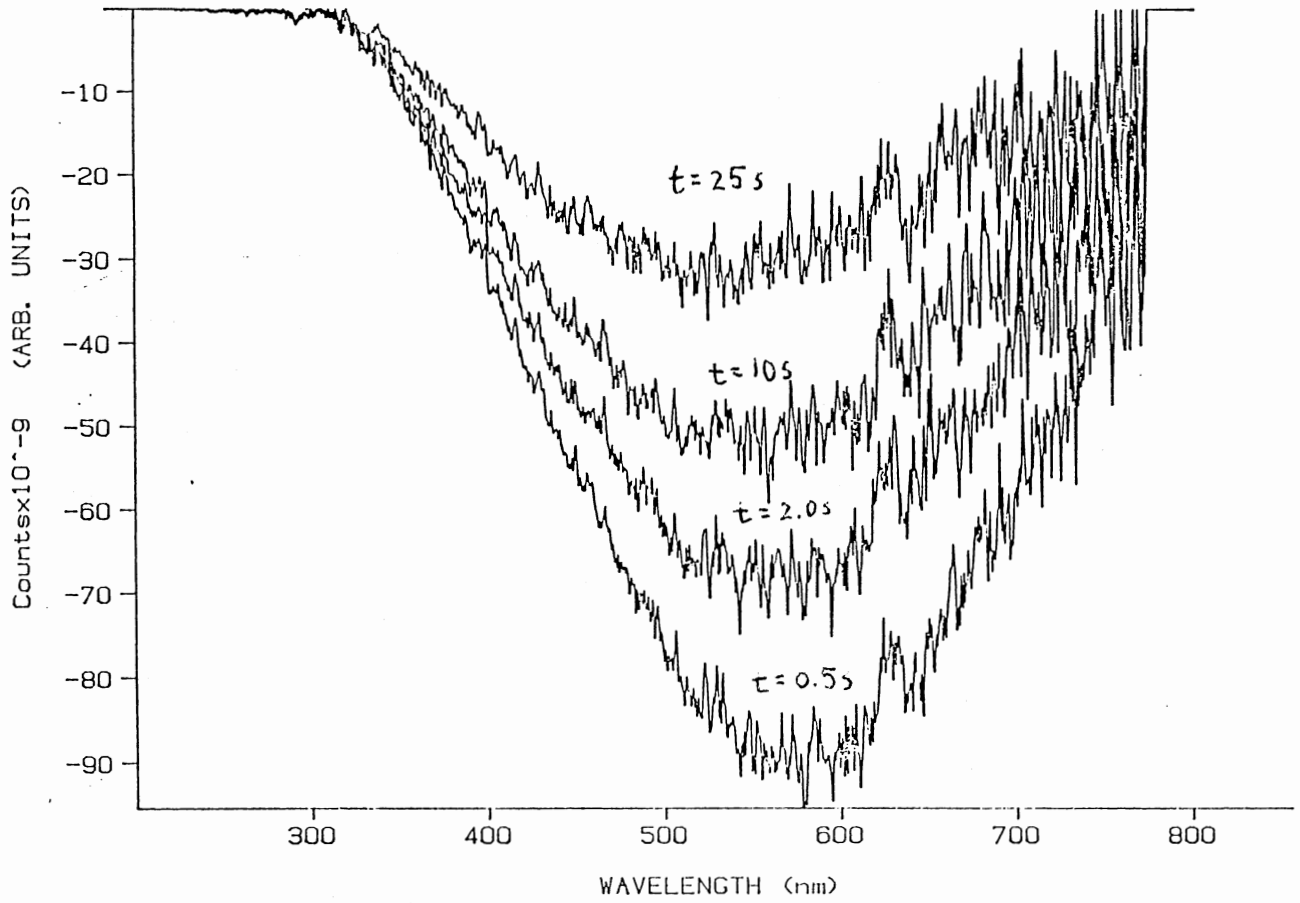

Figure 10. Decay of the 550 nm optical absorption band at 300 K for 5% magnesium-doped lithium niobate.

out of the ninety exposures that were accumulated during the decay of the broad absorption band. Following the procedures outlined in the previous chapter, we obtained the graph of the natural logarithm of absorption versus time. It is shown in Figure 11. It closely approximates a straight line and this indicates that, to a good approximation, the absorption decays exponentially with time.

Additional sets of data similar to those in Figures 10 and 11 were obtained when the sample was irradiated at various temperatures between 200 K and 500 K. An Arrhenius plot of the resulting lifetime versus temperature data is shown in Figure 12. The computer program listed in Figure 9 was used to fit these experimental data and calculate the activation energy. In the temperature range from 200 K to 500 K, the 550 nm optical absorption band has an activation energy of 0.20 eV.

The effect of the intensity of the tungsten lamp on the lifetime of the optical absorption band at 550 nm was investigated. The lamp intensity as seen by the sample was changed by inserting a neutral density filter between the lamp and the sample. The results for a sample temperature of 300 K are shown in Figure 13 and indicate that the lifetime increases on the order of twenty percent as the lamp intensity decreases. This indicates that the defect responsible for the 550 nm optical absorption band is slightly photosensitive and that the tungsten lamp is capable of bleaching the defect center.

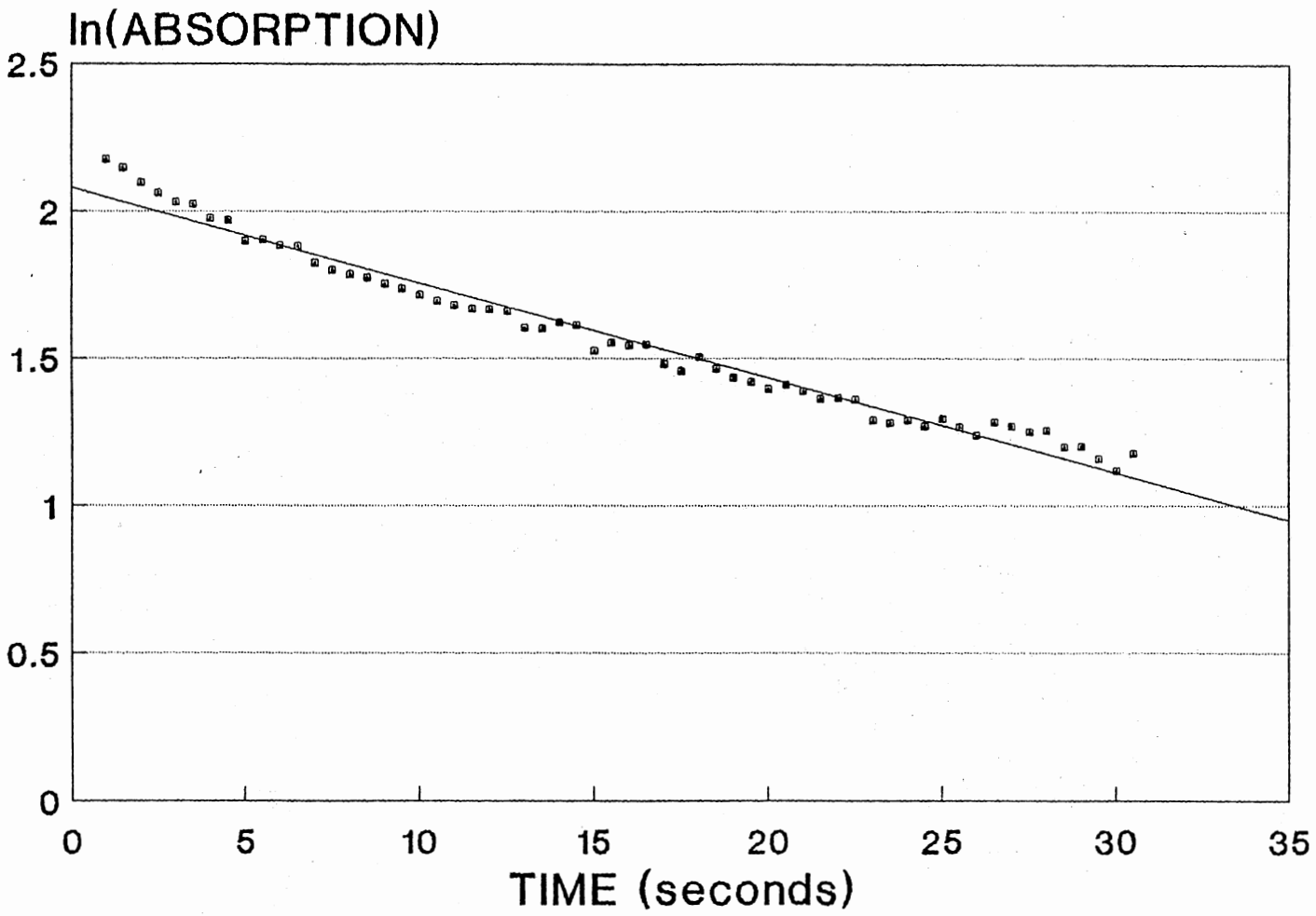

Figure 11. Natural logarithm of absorption versus time for the 550 nm optical absorption band in 5% magnesium-doped lithium niobate.

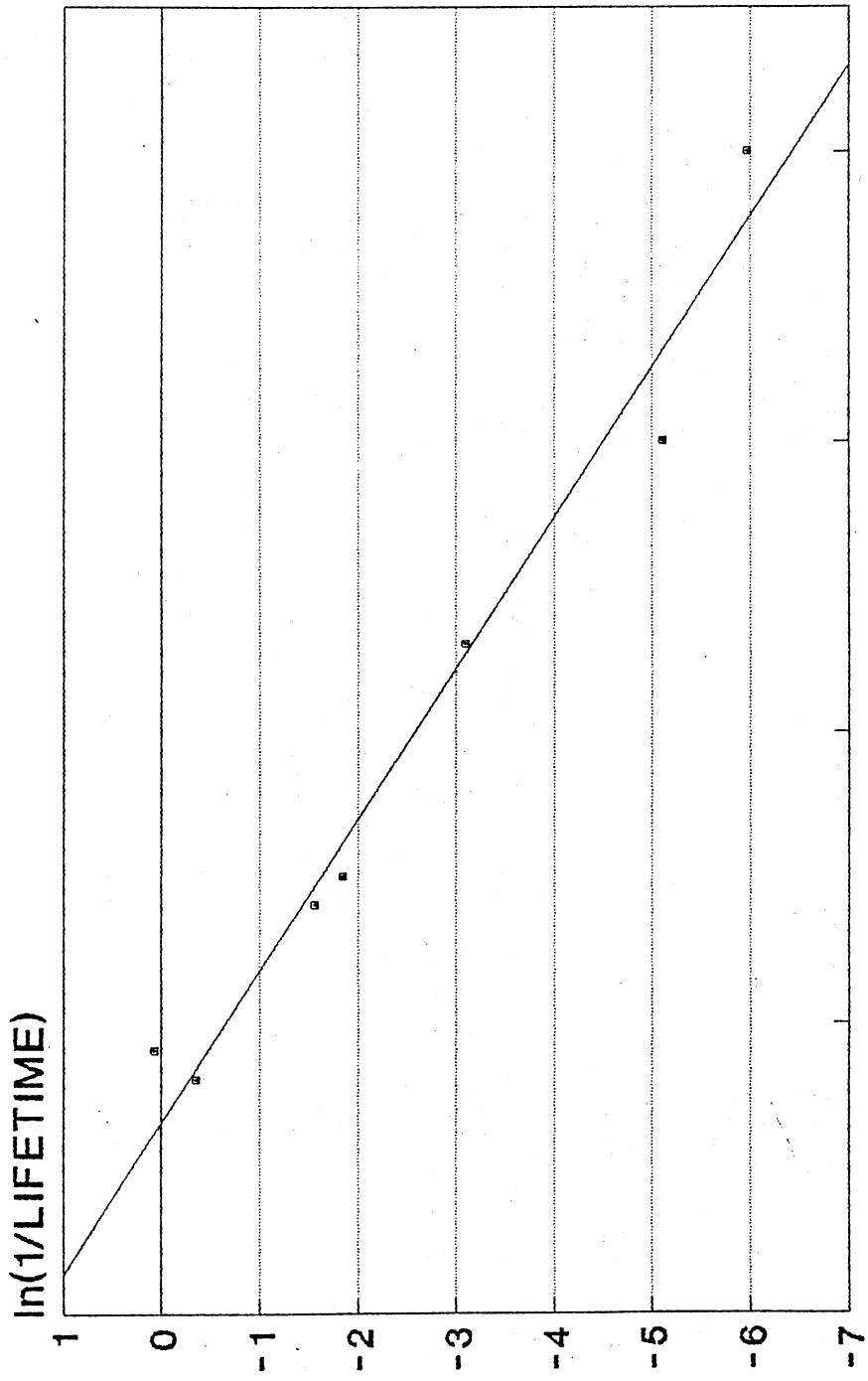

Figure 12. Arrhenius plot of lifetime versus temperature data above 200 K.

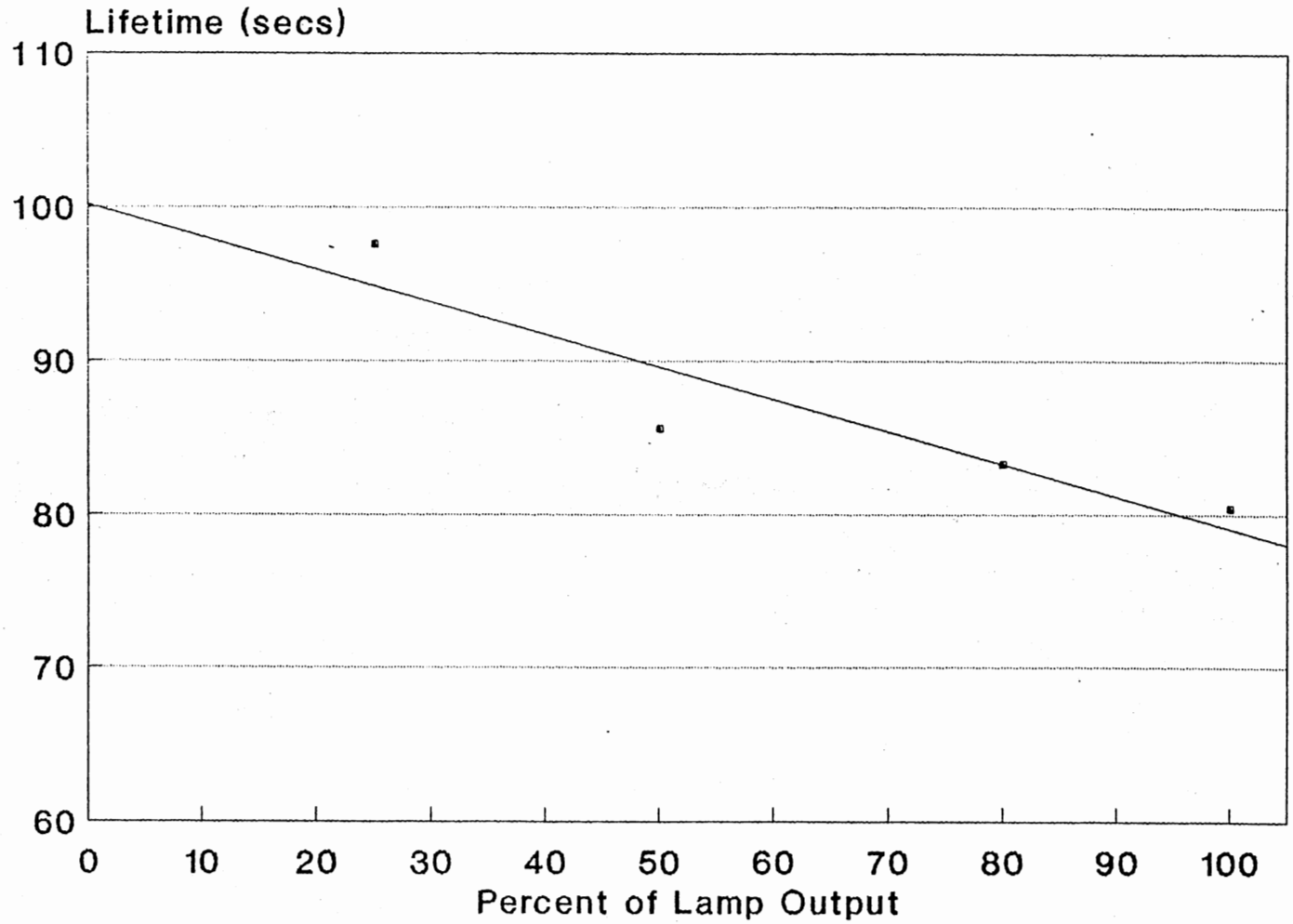

Figure 13. Effect of lamp intensity of lifetime of decay for the 550 nm band at 300 K for 5% magnesium-doped lithium niobate.

Halliburton et al. [18], in a previous study, used optical absorption and electron spin resonance techniques to investigate the effects of ionizing radiation on undoped lithium niobate at 77 K. They observed a broad optical absorption band peaking near 500 nm following a room temperature irradiation. Under similar conditions, electron spin resonance revealed the presence of a spectrum due to trapped holes and a separate spectrum due to electrons trapped at Nb^{4+} ions. The 500-nm absorption band is assigned to the trapped holes. From a pulsed anneal study, it was shown that the optical absorption band and the ESR spectra thermally decayed in the 100 to 300 K range.

The experimental results and previous work suggest the following defect model for the transient optical absorption band peaking near 550 nm observed above 200 K. In our experiment, the high-energy electrons produce free electrons and holes throughout the crystal. The free electrons are captured by the Nb^{5+} to form Nb^{4+} but this defect has no major absorption band associated with it. The hole becomes trapped on an oxygen ion which gives rise to the optical absorption band at 550 nm. The slight photosensitivity described above is probably due to the release of holes.

Bryan et al. [20] investigated the temperature dependence of the photoconductivity and the diffraction efficiency of magnesium-doped lithium niobate over the temperature range from 285 K to 400 K. They report that the photoconductivity and diffraction efficiency show an Arrhenius

dependence on temperature with activation energies of 0.1 to 0.2 eV and 0.1 eV, respectively.

Transient Optical Absorption Below 200 K

Transient optical absorption bands near 1200 nm and 550 nm are observed when the sample is irradiated below a temperature of approximately 200 K. The decay of the 1200 nm optical absorption band, as measured with a photomultiplier tube at a temperature of 23 K, is shown in Figure 14. The large spike in this figure is probably the result of the ionization of the air around the cryostat head. The time decay of the 550 nm optical absorption bands, as measured with the OMA III following an irradiation at 50 K, is shown in Figure 15. Note that the absorption near 750 nm in Figure 15 is due to the tail of the 1200 nm band. This latter absorption decays away faster than the 550 nm absorption band and is explainable in terms of one electron trap converting into another.

The sample was irradiated at various temperatures between 200 K and 50 K. Following each pulse of high-energy electrons, optical absorption data were recorded as a function of time. As in the previous cases, these raw data were converted to lifetimes. An Arrhenius plot of these lifetime and temperature values is shown in Figure 16 for each absorption band. After the absorption data were collected for a particular temperature, the sample was heated to above 290 K and annealed at this temperature for at least five

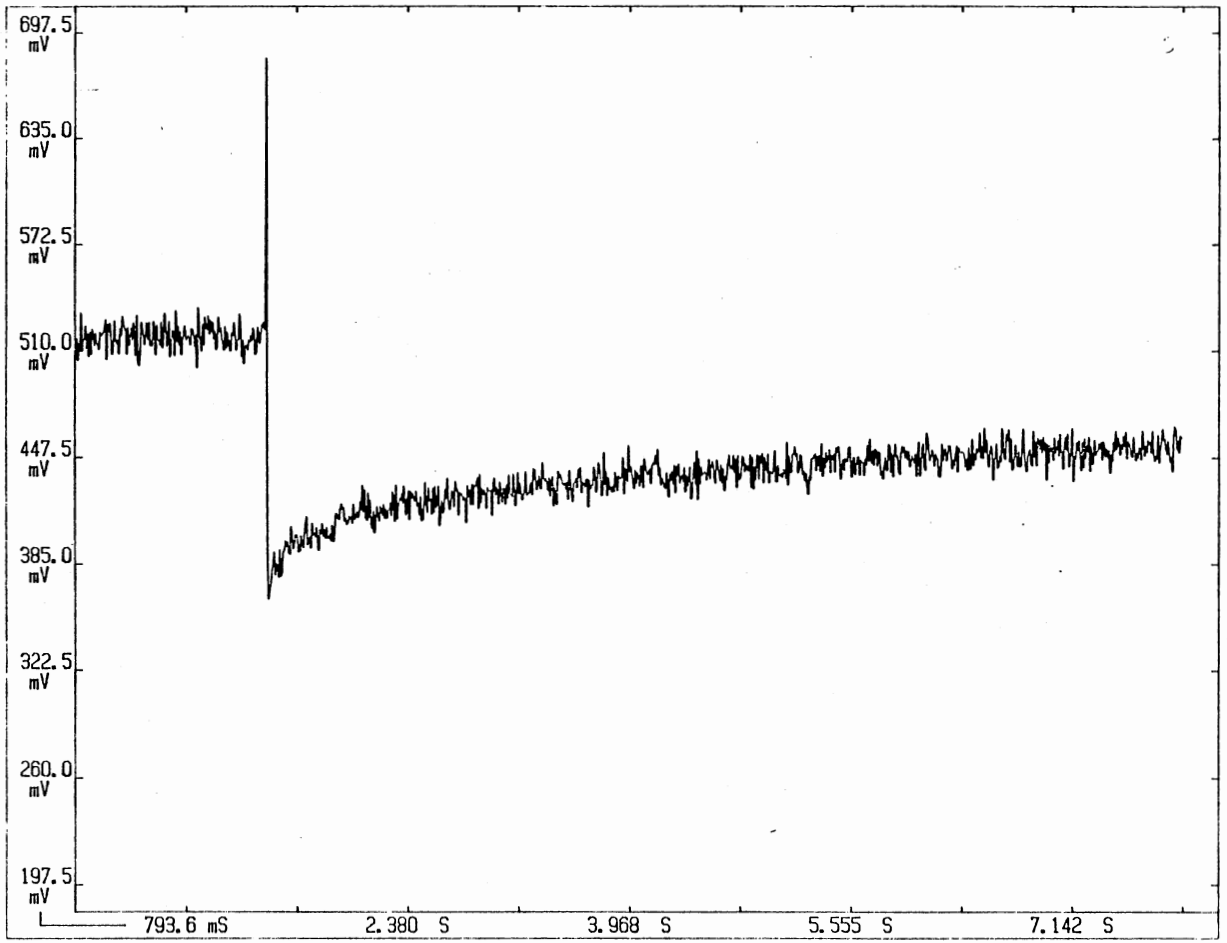

Figure 14. Decay of the 1200 nm optical absorption band at 23 K for 5% magnesium-doped lithium niobate.

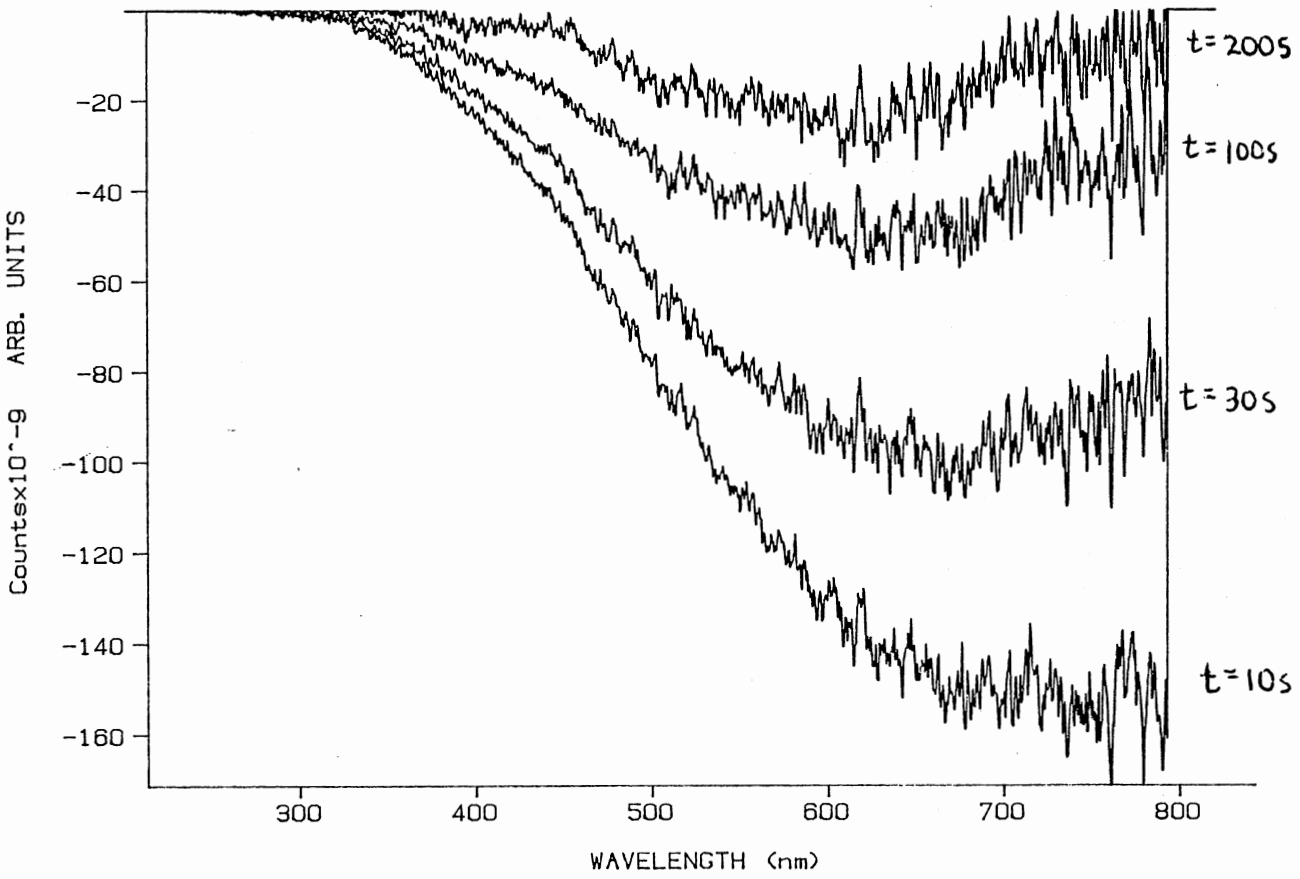

Figure 15. Decay of the 550 nm and 750 nm optical absorption band at 50 K for 5% magnesium-doped lithium niobate.

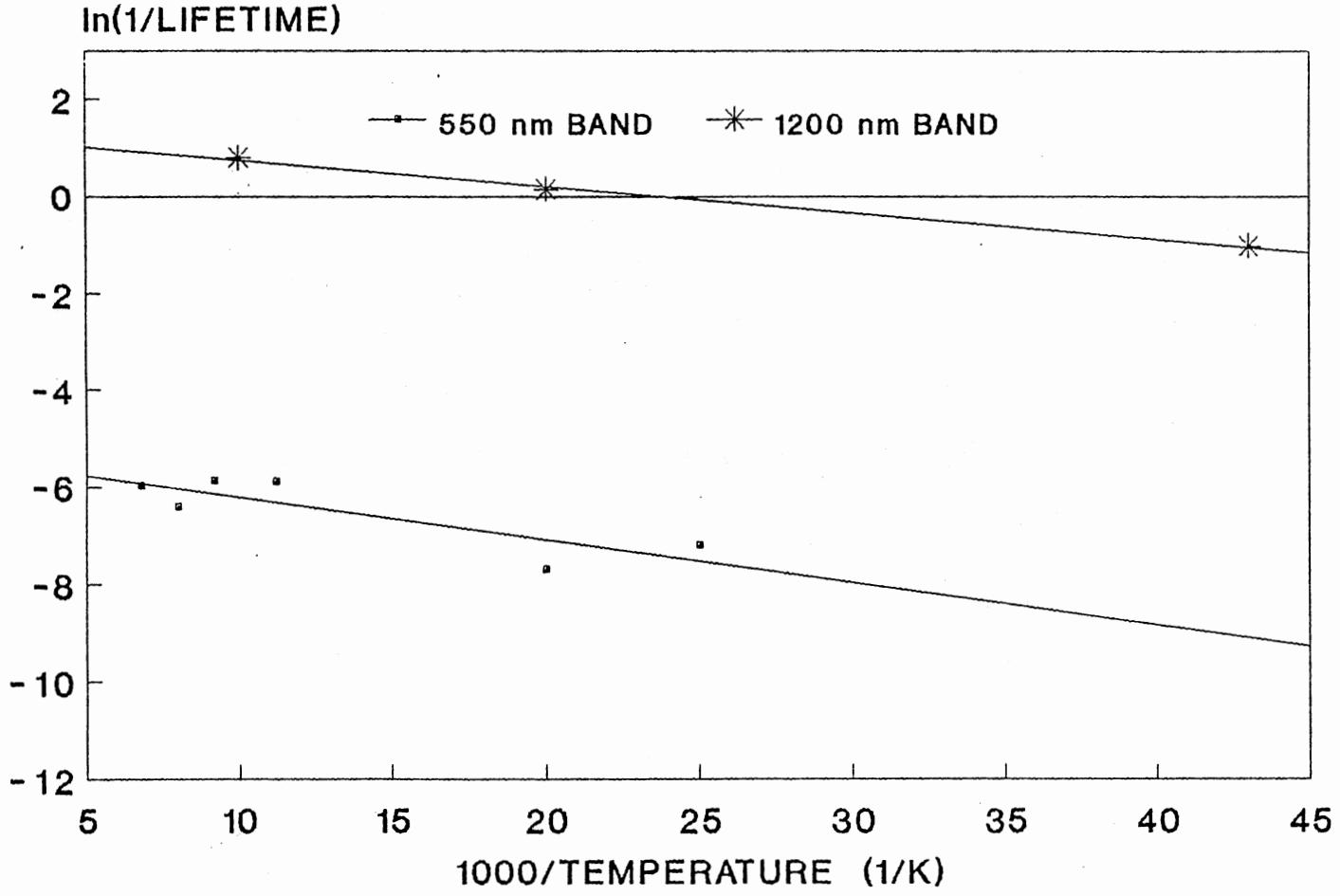

Figure 16. Arrhenius plot of lifetime versus temperature data below 200 K.

minutes in order to free any remaining trapped electrons and holes before preceding to the next irradiation.

The activation energy for an optical absorption band is directly proportional to the slope of the line in the Arrhenius plot shown in Figures 12 and 16. The computer program listed in Figure 9 was used to fit the experimental data and calculate the activation energies. For the temperature range from 200 K to 40 K, the 1200 nm optical absorption band has an activation energy of 0.01 eV and the 550 nm optical absorption band has an activation energy of 0.01 eV. The activation energies for the low temperature 550 nm band and the 1200 nm band are the same within the experimental error limits and this suggests they arise from complementary hole and electron traps.

The experimental results obtained from irradiations below 200 K suggest the following defect model. A pulse of high energy electrons forms free electrons and holes within the lithium niobate sample. Magnesium complexes trap electrons and give rise to the 1200 nm optical absorption band. Sweeney et al. [20] have previously suggested that Mg^{2+} ions may trap electrons. Holes drift to existing defects; for example, a lithium vacancy, where they are captured by an adjacent oxygen ion [20]. This trapped hole center gives rise to the 550 nm absorption band.

CHAPTER V

SUMMARY

Transient optical absorption is observed in magnesium-doped lithium niobate following an irradiation by a pulse of high-energy electrons. These optical absorption bands decay with time even at temperatures below 40 K. Table II summarizes the wavelengths of the absorption peaks, their activation energies, and the probable defect giving rise to the absorption bands.

Irradiation of magnesium-doped lithium niobate above a temperature of 200 K traps holes at oxygen ions which gives rise to a broad optical absorption band peaking near 550 nm. Niobium acts as the electron trap. The tungsten lamp used as a light source in this experiment bleaches one or both of these defects. This implies that the lifetimes shown in Figure 12 do not accurately describe the decay process alone, but that the lifetimes appear shorter because of the bleaching effect.

Irradiations of magnesium-doped lithium niobate below a temperature of 200 K produces two optical absorption bands. Electrons are trapped by the Mg^{2+} ions and give rise to the 1200 nm band. Holes are trapped at oxygen ions and form the 550 nm absorption band.

TABLE II

SUMMARY OF TRANSIENT OPTICAL ABSORPTION RESULTS
IN 5% MAGNESIUM-DOPED LITHIUM NIOBATE

Temperature	Absorption Peak	Activation Energy	Defect
Above 200 K	550 nm	0.20 eV	$O^{2-} + h^{+}$
Below 200 K	550 nm	0.01 eV	$O^{2-} + h^{+}$
	1200 nm	0.01 eV	$Mg^{2+} + e^{-}$

REFERENCES

1. Iizuka, K., Engineering Optics (Springer-Verlag, New York 1985).

2. Glass, A. M., Opt. Eng. 17, 470 (1978).

3. Yariv, A., Quantum Electronics (John Wiley & Sons, New York 1975).

4. Fan, T. Y., A. Cordova-Plaza, M. J. Digonnet, R. L. Byer, and H. J. Shaw, J. Opt. Soc. Am. B3, 140 (1986).

5. Zachariasen, W. H., Skr. Norske Vid.-Ada., Oslo, Mat. Naturv. No. 4 (1928).

6. Ballman, A. A., J. Am. Ceram. Soc. 48, 112 (1965).

7. Carruthers, J. R., G. E. Peterson, M. Grasso, and P. M. Bridenbaugh, J. Appl. Phys. 42, 1846 (1971).

8. Chow, K., H. G. McKnight and L. R. Rothrock, Mat. Res. Bull. 9, 1067 (1971).

9. Rauber, A. in: Curreny Topics in Materials Science, Vol. 1 ed. E. Kaldis, (North-Holland, Amsterdam, 1978) pp. 481-601.

10. Weis, R. S., T. K. Gaylord, Appl. Phys. A37, 191 (1985).

11. Chen, F. S., J. Appl. Phys. 40, 3389 (1969).

12. Bryan, D. A., R. Gerson, and H. E. Tomaschke, Appl. Phys. Lett. 44, 847 (1984).

13. Holman, R. L., P. J. Cressman, and J. F. Revelli, Appl. Phys. Lett. 32, 280 (1978).

14. Feisst, A., P. Koidl, Appl. Phys. Lett. 47, 1125 (1985).

15. Armstrong, J. A., N. Bloembergen, J. Ducuing, and P. Pershan, Phys. Rev. 127, 1918 (1962).

16. Holman, R. L., and P. J. Cressman, IEEE-CHMT 4, 332 (1981).

17. Koechner, W., Solid-State Laser Engineering (Springer-Verlag, New York 1988) pg. 53.

18. Halliburton, L. E., K. L. Sweeney and C. Y. Chen, NVC. Inst. Phys. Res. B1, 344 (1984).

19. Bryan, D. A., R. R. Rice, R. Gerson, H. E. Tomaschke, K. L. Sweeney and L. E. Halliburton, Opt. Eng. 24, 140 (1985).

20. Sweeney, K. L., L. E. Halliburton, D. A. Bryan, R. R. Rice, R. Gerson, and H. E. Tomaschke, J. Appl. Phys. Lett. 47, 1036 (1985).

VITA

Donald James Davis

Candidate for the Degree of

Master of Science

Thesis: TRANSIENT OPTICAL ABSORPTION IN MAGNESIUM-DOPED LITHIUM NIOBATE

Major Field: Physics

Biographical:

Personal Data: Born in Youngstown, Ohio, November 17, 1964, the son of Robert L. and Barbara M. Davis. Married Pamela A. Bodosky on December 26, 1987.

Education: Graduated with Honors from Conneaut Lake Area High School, Conneaut Lake, Pennsylvania in 1983; received Bachelor of Arts Degree in Physics with Honors from Thiel College, Greenville, Pennsylvania in May, 1987; completed requirements for the Master of Science degree at Oklahoma State University in July, 1989.

Experience: Departmental Assistant, Department of Physics, Thiel College, September, 1982 to June, 1987; Metallurgical Laboratory Technician, R. D. Werner Company, August, 1985 to June, 1987; Graduate Research Assistant/Graduate Teaching Assistant, Department of Physics, Oklahoma State University, June, 1987 to July, 1989. Member of the Sigma Pi Sigma honor society, the International Society for Optical Engineering, and the Optical Society of America.